

The influence of particle size and interactions on the magnetization and susceptibility of nanometre-size particles

M Hanson†, C Johansson†, M S Pedersen‡ and S Mørup‡

† Physics Department, Chalmers University of Technology and Göteborg University, S-412 96 Göteborg, Sweden

‡ Physics Department, Building 307, Technical University of Denmark, DK-2800, Lyngby, Denmark

Received 26 June 1995, in final form 22 September 1995

Abstract. We studied the magnetic properties of frozen magnetic liquids containing amorphous $\text{Fe}_{1-x}\text{C}_x$ particles. By varying the particle size and concentration, we could separate single-particle effects from interactions. In samples containing particles with median diameters 5.0 nm and 3.8 nm and with spontaneous saturation magnetizations 7.1 kA m^{-1} and 9.2 kA m^{-1} , effects of particle interactions are observed. For 3.2 nm no interactions were observed. In samples with negligible interactions the superparamagnetic blocking temperature increases with the particle size. The effective anisotropy constant increases with decreasing particle size, implying that the anisotropy is enhanced by surface effects.

1. Introduction

Small magnetic particles are the building blocks of many magnetic materials, and it is of fundamental interest to study their physical properties. For single-domain particles the Néel model [1] of superparamagnetism has frequently been used to describe their magnetic behaviour (see for instance the early review by Bean and Livingston [2]). In this model each particle is ascribed a permanent magnetic moment, that changes direction due to thermal fluctuations. In thermodynamic equilibrium the magnetization of an ensemble of such identical, non-interacting, randomly distributed particles is given by the Langevin function and the initial susceptibility obeys a Curie law. Real particle ensembles invariably deviate from the ideal superparamagnetic behaviour in experiments. One reason for this is that there are interparticle interactions, which depend upon the size and size distribution of the particles, the magnetic moments of the particles and the distances between them. In order to separate interactions from single-particle behaviour, it is important to study systems in which particle sizes and distances may be varied independently of each other. These conditions are normally not fulfilled, since most preparation methods lead to broad particle size distributions and particle separations that vary considerably. Magnetic liquids prepared by thermal decomposition of $\text{Fe}(\text{CO})_5$ in organic liquids are, however, excellent modelling systems for studies of the physical properties of ultrafine particles [3–9]. The size of the particles is determined by the surfactant used in the decomposition process, and, by choosing the appropriate surfactant molecules, it is possible to vary the particle diameters between 3 nm and 6 nm, with narrow size distributions. The coated particles are well dispersed in the carrier liquid and their concentration may be continuously varied by dilution. In this paper we present results from a study of such liquids, in which we were able to separate single-particle effects from interaction effects.

2. Experimental techniques

2.1. Magnetic liquids

We prepared one liquid, A, with oleyl-sarcosine as surfactant molecules and another, B, with oleic acid. The carrier liquids were hexadecane and decalin, respectively. The size of the particles was estimated from transmission electron micrographs [6, 10]. The diameters have a log-normal size distribution. The median diameter and standard deviation of the particles were estimated as $D_v = 5.0$ nm and $\sigma = 1.0$ nm in liquid A and $D_v = 3.8$ nm and $\sigma = 0.4$ nm in liquid B. We further investigated a liquid C, prepared earlier [6]. In this the carrier liquid is decalin, the surfactant molecules oleic acid and the particle size is given by $D_v = 3.2$ nm and $\sigma = 0.3$ nm.

2.2. Mössbauer spectroscopy

The magnetic particles in the liquids were investigated by Mössbauer spectroscopy. Mössbauer spectra were obtained using a constant-acceleration spectrometer with a 50 mCi source of ^{57}Co in rhodium. Isomer shifts are given relative to that of $\alpha\text{-Fe}$ at room temperature.

2.3. Magnetic measurements

We measured the static magnetization of the liquids with an Oxford Instruments vibrating sample magnetometer in magnetic fields, B , up to 12 T. The measurements were made on frozen samples in the temperature range $10\text{ K} \leq T \leq 250\text{ K}$, where the magnetization of a particle changes direction by Néel rotation. To obtain the initial susceptibility, χ_i , the samples were cooled in zero field to a preset temperature, and the magnetization measured in the range $-0.01\text{ T} \leq B \leq 0.01\text{ T}$. Thereafter the samples were successively warmed to higher temperatures, and the magnetization measured in the same range of fields. The zero-field cooled magnetization, M_{ZFC} , was measured on samples that were initially cooled in zero field from room temperature to 10 K. Then a field of 0.002 T was applied, and the magnetization measured in constant field during warming. To obtain the field cooled magnetization, M_{FC} , the samples were cooled in zero field from room temperature to 200 K. This is well below the melting points of the liquids. No time dependence or remanence was observed in the magnetization at this temperature, which ascertains that 200 K is above any superparamagnetic blocking temperature of the particles. Then a constant field of 0.002 T was applied, and the magnetization measured during cooling down to 10 K. The cooling and warming rates were 0.05 K s^{-1} . The magnetization of the liquids increases with field without saturation up to 12 T, with a high-field susceptibility that is independent of particle size. This is interpreted as an intrinsic volume effect in the particles due to their amorphous structure [11], and gives further evidence that all particles have the same composition and structure. The spontaneous saturation magnetization, M_0 , was obtained by extrapolating the high-field data to zero field [6, 11]. The values at 200 K for liquids A, B and C were $M_0 = 7.1\text{ kA m}^{-1}$, 9.2 kA m^{-1} and 21.0 kA m^{-1} , respectively. Thus, the liquids contain similar volume fractions of magnetic material. Three additional liquids were prepared by diluting liquid A about 10 and 20 times, which yielded $M_0 = 0.7\text{ kA m}^{-1}$ and 0.3 kA m^{-1} , and liquid B about 20 times, which yielded $M_0 = 0.4\text{ kA m}^{-1}$. Liquid C was diluted about three times and 30 times, yielding $M_0 = 7\text{ kA m}^{-1}$ and 0.7 kA m^{-1} . The fact that the spontaneous saturation magnetization of the liquids is proportional to the concentration of magnetic particles ascertains that no oxidation has taken place during the dilution.

3. Results and discussion

3.1. Mössbauer spectra

In figure 1 a Mössbauer spectrum of liquid A obtained at 15 K and in zero applied field is shown. The absorption lines in the spectra were fitted to Lorentzian lines by a least-squares method. For all three liquids an average hyperfine field of (27 ± 1) T and an isomer shift of (0.35 ± 0.05) mm s⁻¹ are found. The quadrupole shifts are negligible. The lines are broadened, showing that the particles in the liquids consist of an amorphous Fe_{1-x}C_x alloy with $x \approx 0.25$ [12]. The small component, about 5% of the spectrum, with a hyperfine field of (47 ± 1) T indicates the presence of a disordered iron oxide. Altogether the Mössbauer measurements show that the structure and composition of all the magnetic particles prepared by this method are very much alike [10]. At 180 K the Mössbauer spectra are significantly affected by superparamagnetic relaxation. The superparamagnetic blocking temperature, T_B^M , taken as the temperature at which 50% of the spectrum is affected by superparamagnetic relaxation, was determined as $130 \text{ K} \pm 50 \text{ K}$ for liquid A and $85 \text{ K} \pm 20 \text{ K}$ for liquid B. For liquid C it is of the order of 80 K [6].

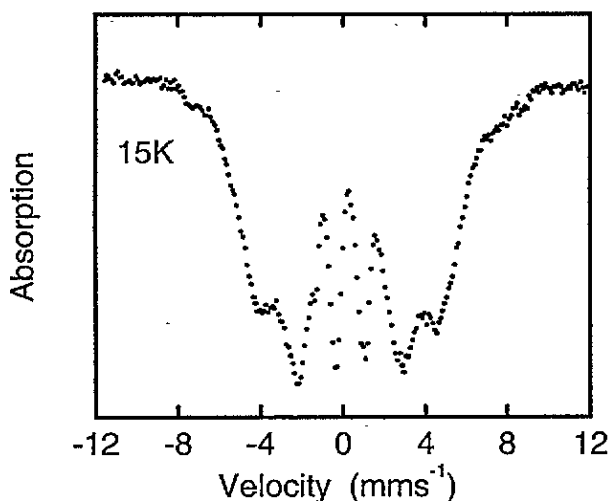


Figure 1. A Mössbauer spectrum of liquid A obtained at 15 K and in zero applied field.

3.2. Zero-field cooled and field cooled magnetization

In figure 2 M_{ZFC} and M_{FC} , normalized to M_0 , are plotted versus temperature for four of the magnetic liquids. They all have a rounded maximum in M_{ZFC} at a temperature T_p within the experimental temperature range. T_p decreases with decreasing particle size. There is also a concentration dependence in T_p , strongest for the liquid with the largest particles, A, weaker for liquid B and negligible for liquid C with the smallest particles (see table 1). M_{FC} increases with decreasing temperature in the whole temperature range. At high temperatures M_{ZFC} and M_{FC} coincide, but, as the temperature approaches T_p from above, the curves begin to diverge at a temperature T_d . The values of T_p and T_d for the liquids are compiled in table 1. T_d indicates the onset of blocking for the largest particles in each liquid. Above this temperature the samples reach thermal equilibrium within the time scale of the magnetic measurements, $\tau_m = 10$ s, i.e. the magnetic particles are superparamagnetic.

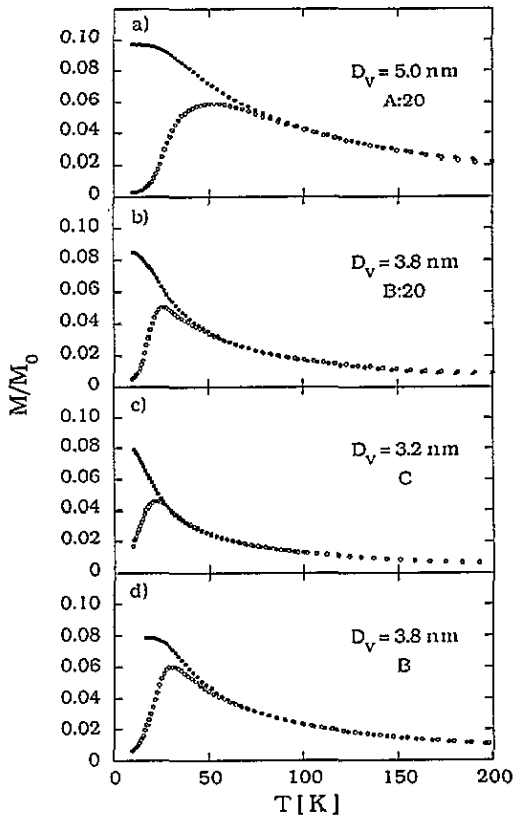


Figure 2. Normalized zero-field cooled magnetization, unfilled circles, and field cooled magnetization, filled circles, versus temperature. The plots are shown for the magnetic liquids A:20, B:20 and C, for which the influence of interactions is negligible, and liquid B which shows clear effects of interactions in the susceptibility (cf. table 1). D_V is the median particle diameter for each liquid.

3.3. Curie-Weiss analysis

In figure 3 the inverse susceptibility, χ_i^{-1} , multiplied by M_0 , is plotted versus temperature in the range well above T_d and still below the melting temperature, T_M , for five of the liquids. There is a linear relation between χ_i^{-1} and T . This is shown in figure 3 by the straight lines obtained by linear regression. For all concentrations of liquid C with the smallest particles, the curves extrapolate to the origin. This corresponds to a Curie law, $\chi_i = C/T$, and indicates that the interactions are negligible in this liquid. For the concentrated liquids A and B, χ_i has a Curie-Weiss dependence, $\chi_i = C/(T - \theta)$, yielding intercepts $\theta = 64$ K and 22 K, respectively. The most diluted samples of these liquids yield $\theta = 0$. Although the temperature range is limited for these samples, the results imply that in the concentrated liquids there are magnetic interactions influencing the magnetization also above the temperature region where the superparamagnetic blocking occurs and that the interactions decrease when the concentration is decreased. From the slopes of the straight lines the magnetic moments of the particles were determined. These values are in good agreement with those calculated from the size determined by electron microscopy and a constant intrinsic magnetization (see table 1). The estimated moments are practically

Table 1. A compilation of magnetic liquid data. D_v is the median particle diameter with standard deviation σ . M_0 is the spontaneous saturation magnetization. T_i is the dipolar interaction temperature for a pair of particles separated by the mean distance, r_m . $T_i = 2\mu_0 m^2 / 4\pi r_m^3 k_B = \mu_0 m M_0 / 2\pi k_B$. T_p is the temperature at the maximum of M_{ZFC} and T_B the temperature at which the particle with the median volume becomes blocked. T_d indicates the onset of blocking. K is the effective anisotropy constant calculated as described in the text. m_{VSM} is the particle moment determined from the magnetic measurements and m_{TEM} the magnetic moment calculated from transmission electron microscopy measurements, using the intrinsic magnetization 1400 kA m^{-1} [5]. θ is the Curie–Weiss temperature.

Liquid	$D_v \pm \sigma$ (nm)	M_0 (kA m^{-1})	T_i (K)	T_p (K)	T_B (K)	T_d (K)	K (10^5 J m^{-3})	m_{VSM} (10^{-20} A m^2)	m_{TEM} (10^{-20} A m^2)	θ (K)
A	5.0 ± 1.0	7.1	7.3	66	—	130	—	7.6 ± 0.6	9.1	64
A:10	5.0 ± 1.0	0.7	0.7	54	23	120	1.3	—	9.1	—
A:20	5.0 ± 1.0	0.3	0.3	53	23	120	1.3	8.8 ± 0.7	9.1	0
B	3.8 ± 0.4	9.2	6.3	30	—	75	—	3.9 ± 0.2	4.0	22
B:20	3.8 ± 0.4	0.4	0.3	26	17	70	2.2	4.2 ± 0.2	4.0	0
C	3.2 ± 0.3	21.0	8.2	22	14	27	3.0	2.7 ± 0.1	2.4	0
C:3	3.2 ± 0.3	7.0	2.6	21	13	26	2.8	2.6 ± 0.1	2.4	0
C:30	3.2 ± 0.3	0.7	0.3	20	13	26	2.8	2.5 ± 0.1	2.4	0

independent of concentration for each particle size. We attribute the small variations to the experimental uncertainty. The concentration independence of the particle moments and the agreement with the results from electron microscopy give further evidence that no oxidation of the particles has taken place in the liquids. The Curie, or Curie–Weiss, analysis of the initial susceptibility clearly demonstrates the increase of particle interactions as the particle size is increased. In the following we discuss the single-particle behaviour in the non-interacting case, liquids with $\theta = 0$, and some effects of particle interactions, liquids with $\theta \neq 0$.

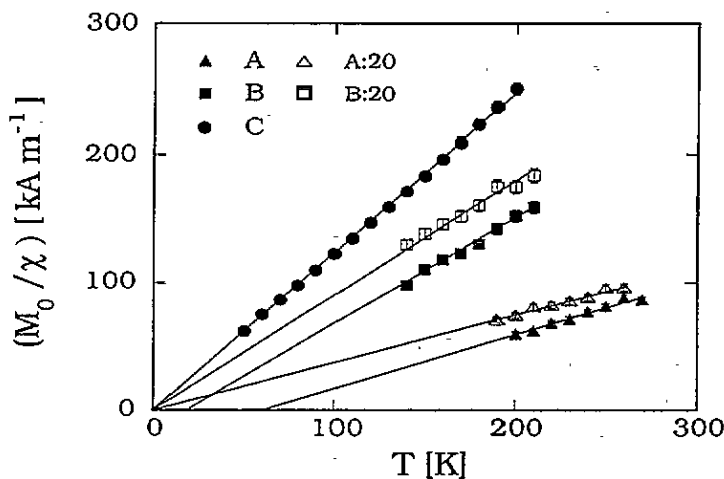


Figure 3. The inverse susceptibility multiplied by the saturation magnetization versus temperature for the magnetic liquids A, B and C with median particle diameters 5.0 nm, 3.8 nm and 3.2 nm respectively. The filled markers indicate the undiluted liquids. The unfilled markers indicate the corresponding most diluted liquids. The error bars in the figure represent a maximal experimental uncertainty of about 3% in the susceptibility values.

3.4. Single-particle effects

In the liquids with $\theta = 0$ the M_{FC} curves continue to increase as T is decreased, well below T_p . The rounded maximum of M_{ZFC} is shifted towards higher temperatures with increasing particle size. These features are characteristic for superparamagnetic blocking of single particles with a size distribution. The value of M_{ZFC} at the lowest temperature, 10 K, is almost zero in liquid A, implying that most particles are blocked. In liquids B and C, with smaller particles, a larger number of particles are still superparamagnetic at 10 K. This behaviour is also reflected in the M_{FC} curves, which become flatter with increasing particle size in the same temperature range. As the blocking temperature, T_B^m , of a particle with volume V we take the temperature at which the experimental measuring time is equal to Néel's relaxation time: $\tau_N = \tau_0 \exp(KV/k_B T)$. K is the uniaxial anisotropy constant and k_B Boltzmann's constant. The main volume and temperature dependence of τ_N is contained in the exponential factor and τ_0 may be treated as a constant. Particles with a distribution of sizes have a distribution of energy barriers, KV . Then T_p may not coincide with the blocking temperature of the median particle volume, V_v [13]. In order to compare different samples we calculated the ratio β between T_p and T_B^m using the actual size distributions [6]. T_B^m was then obtained from $T_B^m = T_p/\beta$, and the anisotropy constant from $K = (k_B T_B^m / V_v) \ln(\tau_m / \tau_0)$. The variation of K over the size distribution is neglected, thus an effective anisotropy constant is obtained. By comparing the blocking temperature for liquid C, as observed in magnetization measurements and in Mössbauer spectroscopy, with an experimental time $\tau_B^m = 2 \times 10^{-9}$ s, we determined a value of $\tau_0 = 2.8 \times 10^{-11}$ s [6]. With this value of τ_0 the values $K = 2.8 \times 10^5$ J m $^{-3}$, 2.2×10^5 J m $^{-3}$ and 1.3×10^5 J m $^{-3}$ were determined for the particles with median diameters $D_v = 3.2$ nm, 3.8 nm and 5.0 nm, respectively. The values are compiled in table 1. As can be seen K is not constant: it increases with decreasing particle size. The anisotropy can also be independently determined from the field dependence of the magnetization at temperatures above the blocking temperature, according to a model including the anisotropy [7]. This yields the same size dependence of K for our particles. Thus we conclude that the anisotropy is not purely a volume effect, but that it also contains considerable contributions from the surface of the particles. Such a size dependence of K has also been found in α -Fe particles, where it was attributed to the influence of surface anisotropy [14].

The estimated values of the anisotropy constants and the actual size distributions were used to calculate the zero-field cooled magnetization of the liquids according to the relation [6]

$$M_{ZFC} = \frac{M_0 \mu_0 I_s H}{V_m 3k_B T} \int_0^{y_B(T)} V^2(y) f_{LN}(y) \frac{dy}{y}. \quad (1)$$

Here V_m is the mean particle volume, μ_0 the permeability of a vacuum, I_s the intrinsic magnetization of the particles and H the applied magnetic field. $V(y)$ is the volume of a particle with diameter $D(y) = y D_v$ and $f_{LN}(y)$ is the log-normal distribution function, given by the relation [15]

$$f_{LN}(y) d(\ln y) = (1/\sqrt{2\pi} \ln \sigma_g) \exp(-(\ln^2 y / 2 \ln^2 \sigma_g)) d(\ln y). \quad (2)$$

Here σ_g is the geometrical standard deviation. The upper limit of integration, $y_B(T)$, is obtained from the volume $V_B(T) = (\pi/6) y_B^3(T) D_v^3$ of the particle that becomes blocked at the actual temperature, according to the relation $\tau_m = \tau_0 \exp(V_B(T)K/k_B T)$. The relations are obtained from the assumption that only particles with T_B below the measuring

temperature contribute to the temperature dependence of the magnetization. In low fields the influence of the anisotropy on the magnetization is small [7], thus it was neglected in the calculations. This simple model with superparamagnetic blocking of single particles gives a good description of the experimental data for all three particle sizes. The fit for the smallest particles was shown in [6].

3.5. Interaction effects

In the liquids with $\theta \neq 0$ the influence of interactions is clearly seen also in the M_{ZFC} and M_{FC} curves. As the concentration is increased, T_p increases and M_{FC} flattens out faster than for the non-interacting liquids below T_p (cf. figure 2(b) and (d)). This behaviour may be qualitatively explained by the presence of dipolar interactions which lead to coupling between the magnetic moments when the temperature is decreased. This slows down the thermal relaxation and prevents alignment of the moments in the small external field. The effects are, however, enhanced for the larger particle sizes, implying that there may be a critical size, between 3.2 nm and 3.8 nm, below which the interactions are negligible. We made an estimate of the dipolar interactions, T_i , between a pair of particles with the mean interparticle separation (cf. table 1). When T_i is compared to the superparamagnetic blocking temperature of the actual liquid, one would expect the interactions to be more important in liquid C than in the others. The experiments, on the contrary, show that the interactions are negligible in C, but influence the magnetic properties of A and B. This suggests that a model in which the interparticle distance is assumed to be equal to the median separation cannot account for the results. Another possibility may be that the interactions influence the geometrical arrangement of the particles in the liquids. The largest pair interaction is obtained for the minimum separation $d_{\min} = D_v + 2l$, where l is the thickness of the surfactant layer. With $l \approx 1.4$ nm for oleyl-sarcosine and 1.1 nm for oleic acid, we obtain the maximum pair interaction yielding ratios of about 3.5:2:1 in A, B and C respectively. If we assume that the particle interactions lead to a non-random distribution, with a number of particles approaching the minimum separation in liquids A and B, the relative strength of the interactions may be qualitatively explained. An indication of the strength of interactions in a fine-particle system can further be obtained from a comparison between the blocking temperatures T_B^m obtained from zero-field cooled magnetization and T_B^M obtained from Mössbauer spectra. For a non-interacting particle system, governed by the Néel relaxation, the ratio between the two blocking temperatures is given by the expression

$$\gamma = T_B^M / T_B^m = \ln(\tau_m / \tau_0) / \ln(\tau_M / \tau_0). \quad (3)$$

When the experiments are made on a sample with a distribution of particle sizes, one must extract the blocking temperatures that are representative of the same particle sizes in both experiments. For liquid C, which has a narrow size distribution and in which the interactions are negligible, we used $T_B^m = T_p / \beta$ to obtain $\tau_0 = 2.8 \times 10^{-11}$ s. With $\tau_M = 2 \times 10^{-9}$ s and $\tau_m = 10$ s, this yields $\gamma = 6$. In particle systems with weak interactions it is observed that the difference between T_B^M and T_B^m decreases [16–20] and the value of γ decreases. For strongly interacting systems, which possibly may order magnetically, the model for superparamagnetic relaxation is no longer applicable and one cannot speak about blocking temperatures. However, we can still compare the ratios between T_B^M and T_p . For the liquids A and B the values of T_B^M / T_p are about 2.0 and 2.8. These values are considerably lower than expected for the non-interacting case [16]. This gives further evidence of the consistency in our interpretation that we can separate single-particle effects and interactions in our particle system.

4. Conclusions

The rounded maximum in M_{ZFC} , observed earlier in magnetic liquids containing iron oxide particles, was interpreted as being due to dipolar interactions [21] or superparamagnetic blocking [22–25]. The influences of interactions and particle sizes were not clearly separated. Among the conditions that may not be fulfilled in the common magnetic liquids with iron oxides, but that made it possible to separate out the single-particle effects in our system, we emphasize the following.

(i) Particles with different sizes can be prepared with sufficiently narrow size distributions to yield a small size overlap between different samples.

(ii) The intrinsic magnetization is independent of particle size.

(iii) The magnetic particles are well dispersed in the liquids.

The main conclusions drawn from the present study of magnetic liquids with amorphous iron-carbon particles are as follows.

(i) By analysing the initial susceptibility according to Curie–Weiss law, we could separate liquids with particle interactions, $\theta \neq 0$, from the non-interacting case, $\theta = 0$.

(ii) The magnetic measurements imply that there is a critical size between 3.2 nm and 3.8 nm, below which particle interactions are negligible.

(iii) In liquids with negligible interactions we observe superparamagnetic relaxation of single particles with a size distribution. For particles with median diameters $D_v = 3.2$ nm, 3.8 nm and 5.0 nm an effective anisotropy constant within the Néel model was determined: $K = 2.8 \times 10^5$ J m⁻³, 2.2×10^5 J m⁻³ and 1.3×10^5 J m⁻³, respectively. From this we conclude that the anisotropy is strongly enhanced by the surface.

(iv) The magnetic interactions between the particles lead to an increase of the temperature at the maximum of the zero-field cooled magnetization.

For the liquid with the smallest particles, 3.2 nm, which has been extensively investigated also in [6, 7, 11, 26], all the results can be interpreted within the same model of single-domain, non-interacting particles with uniaxial anisotropy. Thus we conclude that Néel's model for superparamagnetic relaxation is adequate for this system.

Acknowledgments

This work was financially supported by the Swedish National Board for Industrial and Technical Development, the Swedish Natural Science Research Council and the Danish Council for Technical Research.

References

- [1] Néel L 1949 *C. R. Acad. Sci. Paris* **228** 664–6
- [2] Bean C P and Livingston J D 1959 *J. Appl. Phys.* **30** S120–9
- [3] Griffiths C H, O'Horo M P and Smith T W 1979 *J. Appl. Phys.* **50** 7108–15
- [4] van Wonerghem J, Mørup S, Charles S W and Wells S 1988 *J. Colloid Interface Sci.* **121** 558–63
- [5] Mørup S, Bødker F, van Wonerghem J, Madsen M B and Bentzon M D 1989 *Hyperfine Interact.* **51** 1071–8
- [6] Johansson C, Hanson M, Hendriksen P V and Mørup S 1993 *J. Magn. Magn. Mater.* **122** 125–8
- [7] Hanson M, Johansson C and Mørup S 1993 *J. Phys.: Condens. Matter* **5** 725–32
- [8] Linderoth S, Balcells L, Labarta A, Tejada J, Hendriksen P V and Sethi S A 1993 *J. Magn. Magn. Mater.* **124** 269–76

- [9] van Wonerghem J, Mørup S, Charles S W, Wells S and Villadsen J 1985 *Phys. Rev. Lett.* **55** 410-3
- [10] Pedersen M S, Mørup S, Sethi S, Hanson M and Johansson C 1994 *Hyperfine Interact.* **93** 1433-7
- [11] Johansson C, Hanson M, Pedersen M S and Mørup S 1994 *J. Magn. Magn. Mater.* **134** 25-8
- [12] Bauer-Grosse E and Le Caer G 1987 *Phil. Mag.* **B 56** 485-500
- [13] Gittleman J J, Abeles B and Bozowski S 1974 *Phys. Rev. B* **9** 3891-7
- [14] Bødker F, Mørup S and Linderøth S 1994 *Phys. Rev. Lett.* **72** 282-5
- [15] Granqvist C G and Buhrman R A 1976 *J. Appl. Phys.* **47** 2200-19
- [16] Mørup S 1994 *Europhys. Lett.* **28** 671-6
- [17] Mørup S and Tronc E 1994 *Phys. Rev. Lett.* **72** 3278-81
- [18] Hendriksen P V, Oxborrow C A, Linderøth S, Mørup S, Hanson M, Johansson C, Bødker F, Davies K, Charles S W and Wells S 1993 *Nucl. Instrum. Methods Phys. Res. B* **76** 138-9
- [19] Mørup S, Bødker F, Hendriksen P V and Linderøth S 1995 *Phys. Rev. B* **52** 287-94
- [20] Mørup S, Oxborrow C A, Hendriksen P V, Pedersen M S, Hanson M and Johansson C 1995 *J. Magn. Magn. Mater.* **140-144** 409-10
- [21] Luo W, Nagel S R, Rosenbaum T F and Rosenweig R E 1991 *Phys. Rev. Lett.* **67** 2721-4
- [22] Cayless A T, Hoon S R, Tanner B K, Chantrell R W and Kilner M 1993 *J. Magn. Magn. Mater.* **30** 303-11
- [23] Tari A, Popplewell J, Charles S W, Bunbury D St P and Alves K M 1983 *J. Appl. Phys.* **54** 3351-8
- [24] Chantrell R W, El-Hilo M and O'Grady K 1991 *IEEE Trans. Magn.* **MAG-27** 3570-8
- [25] Ayoub N Y 1991 *Japan. J. Appl. Phys.* **30** 3381-5
- [26] Hanson M, Johansson C and Mørup S 1995 *J. Phys.: Condens. Matter* **7** 9263-8